Local Pressure-Induced Metallization of a Semiconducting Carbon Nanotube in a Crossed Junction

L. Vitali, M. Burghard, P. Wahl, M. A. Schneider, and K. Kern

Max-Planck-Institut für Festkörperforschung, Heisenbergstrasse 1, D-70569 Stuttgart, Germany

(Received 23 May 2005; published 3 March 2006)

The electronic and vibrational density of states of a semiconducting carbon nanotube in a crossed junction was investigated by elastic and inelastic scanning tunneling spectroscopy. The strong radial compression of the nanotube at the junction induces local metallization spatially confined to a few nanometers. The local electronic modifications are correlated with the observed changes in the radial breathing and *G* band phonon modes, which react very sensitively to local mechanical deformation. In addition, the experiments reveal the crucial contribution of the image charges to the contact potential at nanotube-metal interfaces.

DOI: 10.1103/PhysRevLett.96.086804 PACS numbers: 73.22.−f, 63.22.+m, 68.37.Ef, 85.35.Kt

Single-wall carbon nanotubes (SWCNTs) are highly attractive components in nanoscale electronics such as high-performance field-effect transistors [1] or electrical interconnects [2]. The successful implementation of advanced device functions into nanotubes will critically depend on the availability of methods that allow us to tune the tubes' electronic properties in a well-defined and spatially controllable manner. One possibility to reach this goal is to use conformational changes, which are well-documented to alter the electronic properties of the nanotubes. Such changes can be induced locally by, e.g., mechanical interactions. When a nanotube encounters topographic obstacles like steps in the substrates, electrode lines, or other nanotubes, deformations like bends or kinks are introduced into the tube which can result in the local formation of tunnel barriers [3,4] or other electronic modifications [5,6]. Alternatively, the tip of an atomic force microscope can be used to alter the electronic structure of a nanotube via mechanical manipulation with spatial control in the nanometer range [7]. In order to take full advantage of nanomechanical interactions to control the electronic properties of nanotubes and thereby to tailor nanodevices, a detailed microscopic understanding of mechanical nanotube contacts is mandatory.

Particularly favorable configurations to study these contacts are crossed junctions between nanotubes. The interaction between the tubes is well-defined and spatially localized. Theoretical calculations predict a delicate interplay between the structural deformation and the electronic properties of the nanotube junction [5,6] with rich physics ranging from band gap modifications through the formation of localized states to metal-semiconductor transitions. Experimentally crossed nanotube junctions can be addressed by scanning tunneling microscopy, but very few studies have been reported so far [8]. Here we report on the simultaneous experimental determination of the local changes in the electronic and vibrational properties in an individual semiconducting SWCNT induced by its bending over a thin SWCNT bundle. The electronic and vibrational response to local mechanical distortions is mapped with atomic resolution via elastic and inelastic tunneling spectroscopy [9]. Both electronic and phonon density of states are found to react very sensitively to local tube deformations. Most remarkably, we demonstrate a local metallization of the semiconducting nanotube at the crossing point.

In our experiments, as-produced HiPco (tubes@Rice) SWCNTs have been ultrasonically dispersed in 1,2-dichloroethane and deposited on Au-mica substrates. The samples have been transferred into an UHV system equipped with a home-built STM, and tunneling experiments performed at 6 K using an iridium tip. Recording the first and the second derivative of the tunneling current allows for spatial mapping of the electronic and vibrational density of states with atomic resolution [9].

A topographic image of the investigated SWCNT crossing a bundle, with an apparent height of 14 Å, is depicted in Fig. 1(b). To identify this tube, the procedure described by Wildöer [10] was followed. Using the energy distance between the first van Hove singularities [0.88 eV, Fig. 1(a)], in combination with the chiral angle [11] obtained from the topographic image [Fig. 1(b)], allows the assignment to the semiconducting (9,2) tube [9]. The line profile, traced in Fig. 1(d), indicates that the tube does not follow closely the contour of the bundle below. Three regions can be distinguished along the tube: in region I the tube lies directly on the gold surface, while in region II it is lifted from the substrate and suspended between the Au surface and the SWCNT bundle. Finally, in region III the tube starts to bend over the bundle. The corresponding topography is schematically illustrated in Fig. 1(d).

Within region III, which contains the intersection point between the (9,2) tube and the bundle, a striking change in the electron density of states is recognized in the color scale map [Fig. 1(a)] and the green dI/dV curve [Fig. 1(c)]. The conductivity at the Fermi level is considerably enhanced, and the original energy gap no longer

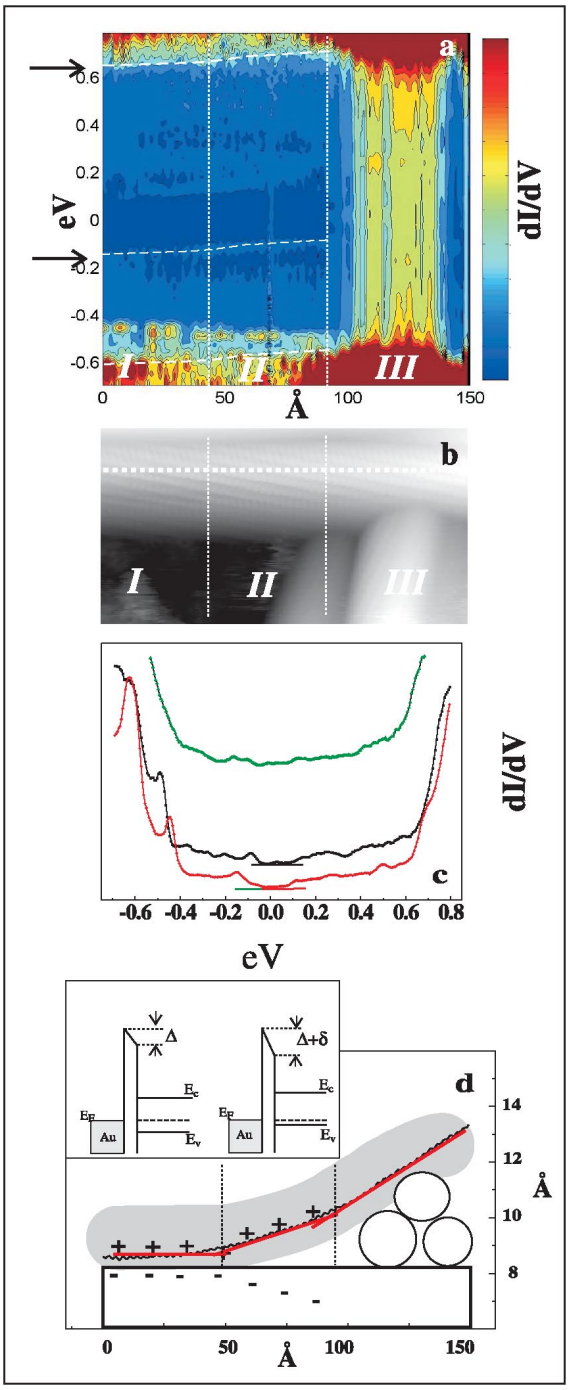

FIG. 1 (color). (a) Local electronic density of states of an (9,2) carbon nanotube crossing a bundle, as revealed by elastic scanning tunneling spectroscopy. The dI/dV signal is measured under open feedback conditions along the tube axis. (b) Topographic STM image of the corresponding nanotube; note that the tube extends for further 150 Å on the right side of the crossing point. (c) Trace lines of the dI/dV at region I (red), II (black), and III (green). The trace line of region II has been shifted for clarity. The color horizontal lines represent the zero dI/dV signal for the respective regions. The large density of state at the Fermi level in region III (green) is characteristic of a metallic character. (d) Schematic description of the tube and the corresponding contact potential. The line on top of the nanotube is the measured line profile along the tube axis.

visible, indicating that the nanotube assumes metallic character in this region. Shortly after the crossing point, the initial semiconducting character of the (9,2) tube is restored, which demonstrates the very local character of the metallization. While previous work reported strong perturbations of the electron density of states and the formation of tunneling barriers as a consequence of tube crossings or interaction with patterned substrates [4,12,13], the local metallization of a semiconducting tube has not yet been observed.

Before discussing in detail this local metallization we first analyze the electronic and vibrational structure of the adsorbed and freely suspended tube segments. Within the suspended region II, it can be seen that the van Hove singularities in the valence and conduction bands experience a shift of approximately 60 meV towards higher energy with respect to their position in region I. This shift occurs mostly within the first 1 nm of region II, which is followed by a much weaker dependence with increasing distance from the substrate. The nanotube-metal substrate interface has been subject of several theoretical investigations [14,15]. According to these, the difference in work function between the two materials leads to charge transfer across the metal-tube interface. The resulting charge accumulation layer in the nanotube and its image charge in the metallic substrate give rise to a contact potential $\Delta = \Delta_{\mathrm{Holes}} - \Delta_{\mathrm{Images}}$ at the interface which affects the alignment of the nanotube bands, causing their displacement towards higher energies [14,15]. In the suspended tube a depletion region, in which the charge accumulated at the nanotube-metal interface slowly decays, could be expected. In order to explain the observed further shift towards higher energies, the logarithmic decay over distances of the charge density in nanotubes [16,17] has to be considered. Because of the ineffective Coulomb screening the charge density in the 3 nm long suspended segment can, in first approximation, be assumed as constant. On the contrary, in the contacted region the charge screening is more effective due to the metallic substrate. Increasing the distance to the substrate weakens the screening effect of the image charges [Fig. 1(d)], and leads to an apparent excess charge on the nanotube and thus to an increased contact potential at the interface $\Delta' = \Delta + \delta$, which shifts the bands further towards higher energies [Figs. 1(c) and 1(d)].

The modified capacitive coupling of the substrate-nanotube-tip system, in the suspended region, can be addressed in analogy to double barrier tunneling junctions [18]. Using the relation $\Delta V = \Delta Q / C_{\mathrm{TS}}$ where ΔV is the voltage shift, ΔQ the fractional charge at the interface, and C_{TS} the tube-substrate capacitance, the unscreened charge can be estimated from the measured shift of the valence band singularity. For the capacitance C, we apply the model of a finite wire of length L at a distance z from a conducting plate $C = 2\pi\epsilon_0\epsilon_r L / \ln(4z/d)$ [19]. Considering the measured energy shift of 60 meV, an averaged tube-substrate distance of 1 nm, a length of 3 nm for the tube section

within which most of the shift occurs, and assuming $\epsilon_r = 2$, the reduced screening is associated with an additional charge of 0.08 holes on the suspended tube segment. Noting that theoretical predictions estimate that, upon bringing the nanotube into contact with a gold surfaces, 0.3 holes are transferred in the same tube length [20], the reduced screening of the image charge is equivalent to an additional 26% of the total charge transferred at the interface. This should be considered as a lower limit of the image-charge contribution to the interface potential since a soft band bending likely counteracts the effect of the reduced screening. This result, however, suggests that the contact potential at the tube-metal interface is determined not only by the difference in the work functions, but also significantly influenced by the image charge. This property places the nanotube interface at an intermediate position between the bulk inorganic semiconductor-metal interface, where the image charge only marginally influences the contact barrier, and the organic semiconductor-metal interface, where the contribution of the image charge is comparable to the built-in potential [21].

The behavior of the most prominent phonon modes, namely, the radial breathing mode (RBM) and the G band are apparent from the corresponding inelastic-electron-tunneling spectroscopy maps (Fig. 2), which display the total phonon density of states as a function of position along the tube axis. In view of the low sensitivity of the G band and of the RBM to charge doping [22,23], it is not expected that the small additional charge in the tube segment of region II ($\sim 1 \times 10^{-4}$ holes per carbon atom) shifts these modes significantly. As can be seen in Fig. 2(a), the G band, which consists of 6 unresolved vibrational modes [24] corresponding to lattice displacements in the circumferential direction (tangential modes) and along the tube axis (longitudinal modes), occurs in region I between 190 and 200 meV. Within region II, the energy position of the longitudinal modes stays constant while a gradual decrease of the intensity of the tangential displacements is observed. A similar observation has been made in case of chemically doped carbon nanotubes [24]. The RBM, which comprises the in-phase radial displacement of the carbon atoms and whose energy scales inversely with the tube diameter occurs on the metal substrate at an energy of 32 meV [see Fig. 2(b)], in good accordance with the value expected for the (9,2) tube with a diameter of 8.1 Å [9]. Within region II, the RBM experiences a slight downshift by about 1.5 meV as compared to region I. This downshift can be attributed to the reduced interaction forces with the substrate as a result of lifting the tube. The importance of the surrounding is well-documented in nanotube bundles, where van der Waals interactions cause stiffening of the RBM [25]. For the (9,2) tube, the RBM is expected to harden by 6% due to these interactions with respect to the freestanding tube. Although the van der Waals interaction of the tube with the surface is not isotropic as in a nanotube bundle, the experimentally observed decrease in the RBM

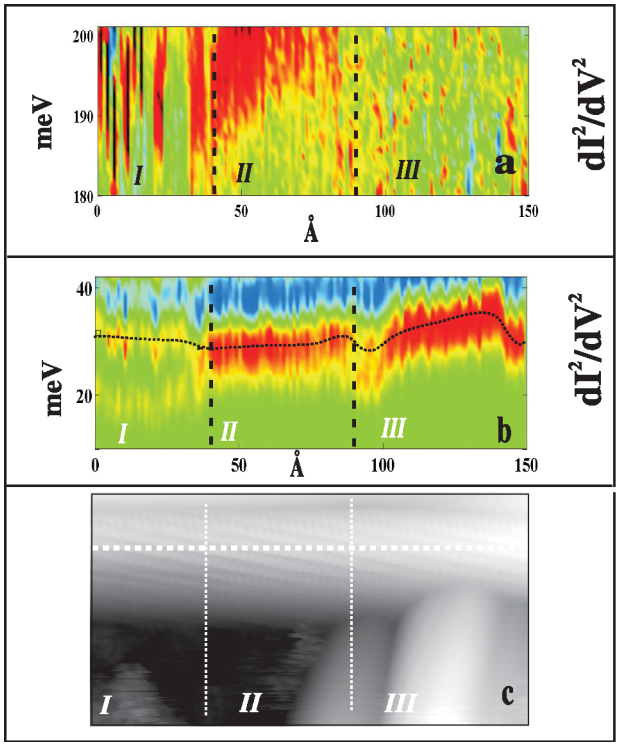

FIG. 2 (color). Local vibrational density of states of the (9,2) carbon nanotube crossing a bundle as revealed by inelastic scanning tunneling spectroscopy. the dI^2/dV^2 signal is measured in open feedback conditions along the tube axis. The region of the tangential mode (a) and the radial breathing mode (b) are displayed; the dotted line (in b) is a guide to the eye. (c) Corresponding STM topography.

energy of 1.5 meV upon entering region II, is largely consistent with the estimated value of 1.9 meV.

The van der Waals forces attracting the tube to the substrate might result in a large local pressure at the crossing region [3]. This can lead to the formation of local defects [6] or to an elliptical tube cross section [3]. In the present case, the line profile [Fig. 1(d)] shows that in region III the total height of the nanotube-bundle system is reduced by 35%. Considering that the diameter distribution in the used HiPco is narrow enough that different compressibility of the tube need not to be considered [26–28], we can assume an homogeneous radial compression of all the tubes at the junction. It is then worth noting that an elliptical tube cross section with axis ratio 0.65 implies that at the crossing point the (9,2) tube has a short axis length comparable to the theoretically predicted 4.6 Å necessary to induce a semiconductor-metal transition [5]. It is therefore likely that the observed tube metallization is induced by the local structural change. Furthermore, the absence of resonant states in the dI/dV spectrum [Figs. 1(a) and 1(c)] excludes the presence of local defects in this region [9]. The compressibility of the tube bundle provides an estimate of the pressure P imposed at the crossing junction through the infinitesimal relation $dP = -B(dV/V)$, where V is the volume and B the bulk modu-

lus. To a first approximation, from a bulk modulus of 35 GPa [29] the pressure necessary to obtain a volume reduction of 35% is estimated to 15 GPa. This pressure is in reasonable agreement with that predicted by first principle calculations [3] for nanotubes at crossing junctions. Although the applied pressure is not isotropic, the estimated value is in qualitative agreement with the observed changes in the phonon density of states. Indeed, the strong deformation of the nanotube at the crossing junction is reflected in the behavior of the phonon density of states in region III. In particular, the G band is completely suppressed within region III [Fig. 2(a)]. This observation agrees well with results from high pressure Raman studies, which demonstrated a strong attenuation of the G band above 10 GPa and its complete vanishing at 20 GPa as a consequence of the strong radial compression of the SWCNTs [30]. The energy of the RBM rises to the value of 37 meV at the crossing point [Fig. 2(b)] and quickly restores afterwards. The observed energy variation of the RBM between the suspended and the compressed region ($\sim$7 meV) is lower than the value expected from Raman investigations reporting an increase by 1.1 meV/GPa. However, it is noticed that the present study addresses effective pressures well above 2 GPa, which represents the maximum that could have so far been investigated by Raman spectroscopy due to the loss of the resonance enhancement. Hence, it cannot be excluded that the energy vs pressure dependence of the RBM would assume a significantly weaker slope in the high pressure regime, or that the nonhydrostatic pressure affects the RBM in a different manner. In Fig. 2(b), one furthermore observes a ''wiggle'' (local minimum) in the energy dependence of the RBM at the left border of region III, where the first and the second tube of the bundle are touching. This behavior further illustrates the extreme sensitivity of nanotube phonon modes to local mechanical interactions.

In conclusion, the combination of elastic and inelastic scanning tunneling spectroscopy techniques has revealed a correlation between changes of the local electron and phonon density of states of a semiconducting SWCNT, induced by the bending of the tube over a thin nanotube bundle. In the suspended tube region, the observed shift of the valence band towards the Fermi energy has been attributed to an effective hole doping resulting from reduced screening of the charge accumulation layer by the metal substrate. Around the crossing point, the tube achieves a metallic character. This striking observation has been attributed to the strong local radial compression, which is corroborated by the observed increase in the RBM energy as well as the complete disappearance G band in this tube region.

[1] S. Heinze, J. Tersoff, and P. Avouris, Appl. Phys. Lett. **83**, 5038 (2003).
[2] J. Kong, E. Yenilmez, T. W. Tombler, W. Kim, H. J. Dai, R. B. Laughlin, L. Liu, C. S. Jayanthi, and S. Y. Wu, Phys. Rev. Lett. **87**, 106801 (2001).
[3] T. Hertel, R. E. Walkup, and P. Avouris, Phys. Rev. B **58**, 13 870 (1998).
[4] A. Bezryadin, A. R. M. Verschueren, S. J. Tans, and C. Dekker, Phys. Rev. Lett. **80**, 4036 (1998).
[5] M. S. C. Mazzoni and H. Chacham, Appl. Phys. Lett. **76**, 1561 (2000).
[6] M. Buongiorno Nardelli and J. Bernholc, Phys. Rev. B **60**, R16338 (1999).
[7] H. W. C. Postma, T. Teepen, Z. Yao, M. Grifoni, and C. Dekker, Science **293**, 76 (2001).
[8] J. W. Janssen, S. G. Lemay, L. P. Kouwenhoven, and C. Dekker, Phys. Rev. B **65**, 115423 (2002).
[9] L. Vitali, M. Burghard, M. A. Schneider, L. Liu, C. Jayanthi, and K. Kern, Phys. Rev. Lett. **93**, 136103 (2004).
[10] J. W. G. Wildoer, L. C. Venema, A. G. Rinzler, R. E. Smalley, and C. Dekker, Nature (London) **391**, 59 (1998).
[11] The chiral angle was corrected from topographic distortion following the procedure described by Venema *et al.* [31].
[12] M. S. Fuhrer *et al.*, Science **288**, 494 (2000).
[13] J. W. Jassen, S. G. Lemay, L. P. Kouwenhoven, and C. Dekker, Phys. Rev. B **65**, 115423 (2002).
[14] Y. Xue and S. Datta, Phys. Rev. Lett. **83**, 4844 (1999).
[15] R. Czerw, B. Foley, D. Tekleab, A. Rubio, P. M. Ajayan, and D. L. Carroll, Phys. Rev. B **66**, 033408 (2002).
[16] F. Lonard and J. Tersoff, Phys. Rev. Lett. **83**, 5174 (1999).
[17] A. A. Odintsov, Phys. Rev. Lett. **85**, 150 (2000).
[18] A. E. Hanna, M. T. Tuominen, and M. Tinkham, Phys. Rev. Lett. **68**, 3228 (1992).
[19] *Carbon Nanotubes: Synthesis, Structure, Properties and Applications*, Topics in applied physics Vol. 80, edited by M. S. Dresselhaus, G. Dresselhaus, and P. Avouris (Springer-Verlag, Berlin, 2001), p. 152.
[20] A. Rubio, D. Snchez-Portal, E. Artacho, P. Ordejn, and J. M. Soler, Phys. Rev. Lett. **82**, 3520 (1999).
[21] M. Knupfer and H. Peisert, Phys. Status Solidi (a) **201**, 1055 (2004).
[22] P. Corio, P. S. Santos, V. W. Brar, G. G. Samsonidze, S. G. Chou, and M. S. Dresselhaus, Chem. Phys. Lett. **370**, 675 (2003).
[23] S. Gupta, M. Hughes, A. H. Windle, and J. Robertson, J. Appl. Phys. **95**, 2038 (2004).
[24] M. S. Dresselhaus and P. C. Eklund, Adv. Phys. **49**, 705 (2000).
[25] L. Henrard, E. Hernández, P. Bernier, and A. Rubio, Phys. Rev. B **60**, R8521 (1999).
[26] The distribution of tube diameter in the used HiPco material is between 0.85 and 1.2 nm.
[27] S. Reich, C. Thomsen, and P. Ordejón, Phys. Rev. B **65**, 153407 (2002).
[28] V. N. Popov, V. V. Dorena, and M. Balkanskib, Solid State Commun. **114**, 395 (2000).
[29] S. M. Sharma, S. Karmakar, S. K. Sikka, P. V. Teredesai, A. K. Sood, A. Govindaraj, and C. N. R. Rao, Phys. Rev. B **63**, 205417 (2001).
[30] I. Loa, J. Raman Spectrosc. **34**, 611 (2003).
[31] L. C. Venema, V. Meunier, Ph. Lambin, and C. Dekker, Phys. Rev. B **61**, 2991 (2000).